Available online at www.sciencedirect.com

ScienceDirect

Energy Procedia 45 (2014) 1107 – 1115

Energy Procedia

68th Conference of the Italian Thermal Machines Engineering Association, ATI2013

Ducted propeller flow analysis by means of a generalized actuator disk model

Rodolfo Bontempo[a], Massimo Cardone[a], Marcello Manna[a,*], Giovanni Vorraro[a]

[a] *Dipartimento di Ingegneria Industriale, Università degli Studi di Napoli Federico II, Via Claudio 21, 80125 Naples, Italy.*

Abstract

The paper presents a generalized semi-analytical actuator disk model as applied to the analysis of the flow around ducted propellers at different operating conditions. The model strongly couples the non-linear actuator disk method of Conway[1] (J. Fluid Mech. 1998; 365: 235-267) and the vortex element method of Martensen[2] (Arch. Rat. Mech. 1959; 3: 235-270) and it returns the exact solution, although in an implicit formulation, for incompressible, axisymmetric and inviscid flows. The solution is made explicit through a semi-analytical procedure developed and validated by Bontempo and Manna[3] (J. Fluid Mech. 2013;728:163-195). Moreover the method duly accounts for non-uniform load radial distribution, slipstream contraction, mutual non-linear interaction between duct and propeller, wake rotation, and ducts of general shape. Thanks to its extremely reduced computational cost it can easily be integrated into design systems based on the repeated analysis scheme of hierarchical type. A comparison between open and ducted rotors is carried out in order to quantify the effects of the duct on the overall performance of the device. Emphasis is given to the appropriate matching between the duct geometry and the propeller load to exploit the benefits that could arise ducting the propeller.

Keywords: Ducted propellers; ducted rotors; ducted actuator disk.

1. Introduction

Ducted propellers consist of a combination of two principal components. The first is an annular wing which can be either symmetric with respect to the rotation axis or asymmetric to accommodate for the wake flow field variations. The second component, i.e. the propeller, differs from a typical open propeller because it has to be designed taking into account the mutual interaction between the duct and the rotor.

In general, there are two main type of ducts: the accelerating (also called the Kort nozzle) and the decelerating duct (also referred to as pumpjet). The former, commonly employed on tugs, trawlers, large tankers and supply vessel, develops a propulsive thrust thus increasing the device efficiency and the inflow velocity of the propeller (for this reason it goes by the name of "accelerating duct"). The second, typically used on fast carrier, yields a negative propulsive thrust with a consequent decrease of the efficiency and of the inflow velocity of the propeller (for this

* Corresponding author. Tel.: +39-081-7683287.
E-mail address: marcello.manna@unina.it

doi:10.1016/j.egypro.2014.01.116

reason it goes by the name of "decelerating duct"). However, thanks to the latter feature, the decelerating duct ensures an high pressure at the rotor inlet thus reducing the danger of cavitation. Since the accelerating duct is the most diffused and studied configuration, in the paper only this kind of duct is analysed.

The early form of ducted propeller was patented by Ludwig Kort in 1924. In this preliminary concept the rotor was installed in a long channel passing through the ship hull. The main drawback of this configuration was the significant increase of the frictional resistance due to the presence of the channel. In the course of the time, the outline of the device was developed by transforming the long channel into the nozzle ring characterizing the present day ducted propellers. Finally, Stipa[4] and Kort[5] experimentally proved the increase of the efficiency which can be obtained by ducting the propeller with an accelerating nozzle.

Although, for many years, the design and/or analysis of ducted propellers was mainly carried out on the basis of extensive experimental campaigns [6–10], several theoretical procedures have also been developed since the pioneering work of Horn[11], and Horn and Amtsberg[12]. Most of these theoretical methods are generally based on the combination of different representations of the velocity field induced by the duct (lumped vortex, thin airfoil theory, panel methods etc.) with the one induced by the rotor (actuator disk, lifting line, lifting surface, boundary element methods, etc.). Some examples are due to: Küchemann and Weber[13], Tachmindji[14], Ordway et al.[15], Morgan[16], Morgan[17], Dyne[18], Ryan and Glover[19], Morgan and Caster[20], Caracostas[21], Tsakonas et al.[22], Van Houten[23], Kerwin et al.[24], Kinnas and Coney[25], Coney[26], Kinnas and Coney[27], Baltazar and Falcão de Campos[28], and Çelik et al.[29]. More recently, computational fluid dynamic (CFD) based methods have also been frequently used to study several aspects of the flow around ducted propellers [30–35].

Although, among the previously mentioned methods, the linearised actuator disk undoubtedly represents the oldest and easiest model used to analyse the flow around a propeller [36,37], it is still widely employed both in its linear [38] and non-linear formulation [1,39,40]. Remarkable examples of ducted propellers modelled through an actuator disk are due to: Dickmann and Weissinger[41], Chaplin[42], Van Gunsteren[43], Gibson and Lewis[44] and Falcão de Campos[45]. Extending to ducted rotors the non-linear actuator disk theory of Conway[1], Bontempo and Manna[3] have recently obtained the exact solution of the flow around a ducted actuator disk. Compared with early literature, the method simultaneously accounts for the proper shape of the slipstream, the rotation of the wake, a variable radial distribution of the load, and ducts of general shape. In section §2, the theoretical foundations of the method are summarized and some meaningful results are presented. Finally in §3, in order to bring out the beneficial effects of the duct on the efficiency, the method is applied to compare the performance of ducted and open propellers. Insight about the matching conditions of the ducted configuration are provided analysing the local flow features at the duct inlet.

2. The non-linear ducted actuator disk flow model

The steady, axysimmetric, incompressible and inviscid flow around a ducted propeller is modelled by means of a non-linear actuator disk with an arbitrary radial distribution of the load. Dealing with rotational symmetry, it is obviously advantageous to introduce a cylindrical coordinate system (ζ, σ, θ) with origin at the centre of the disk and with the ζ axis pointed in the free-stream velocity U_∞ direction. Moreover, the flow being axysimmetric, the problem can be best formulated in terms of the Stokes stream function Ψ whose definition is

$$u + U_\infty = \frac{1}{\sigma}\frac{\partial \Psi}{\partial \sigma}, \qquad v = -\frac{1}{\sigma}\frac{\partial \Psi}{\partial \zeta}, \tag{1}$$

where $\boldsymbol{u} = (u, v, w)$ is the velocity vector. Substituting equation (1) in the definition of the θ-component of the vorticity ω_θ yields the following governing equation for the through-flow [39,46]:

$$\frac{\partial^2 \Psi}{\partial \sigma^2} - \frac{1}{\sigma}\frac{\partial \Psi}{\partial \sigma} + \frac{\partial^2 \Psi}{\partial \zeta^2} = -\omega_\theta \sigma. \tag{2}$$

Outside the wake, the tangential component of the vorticity ω_θ, appearing in equation (2), is obviously zero, while inside the slipstream it can be related to the propeller load $\mathcal{H}(\Psi) = \Delta H_{\text{across the disk}} = H(\Psi)|_{(\zeta>0,\sigma<\sigma_s)} - H_\infty$ by means of the momentum equation which, neglecting the body forces, reads

$$\boldsymbol{u} \times \boldsymbol{\omega} = \boldsymbol{\nabla} H, \tag{3}$$

where $H = p/\rho + \left(u^2 + v^2 + w^2\right)/2$. In particular, with some remarkable algebra, the θ-component of the vorticity ω_θ can be expressed as [39]

$$-\omega_\theta \sigma = \begin{cases} \dfrac{\Omega^2\sigma^2 - \mathcal{H}}{\Omega^2}\dfrac{\mathrm{d}\mathcal{H}}{\mathrm{d}\Psi} & \text{inside the slipstream,} \\ 0 & \text{outside the slipstream,} \end{cases} \tag{4}$$

where Ω is the angular velocity of the rotor. Substituting equation (4) in (2) leads to the following form of the governing equation:

$$\frac{\partial^2\Psi}{\partial\sigma^2} - \frac{1}{\sigma}\frac{\partial\Psi}{\partial\sigma} + \frac{\partial^2\Psi}{\partial\zeta^2} = \begin{cases} \dfrac{\Omega^2\sigma^2 - \mathcal{H}}{\Omega^2}\dfrac{\mathrm{d}\mathcal{H}}{\mathrm{d}\Psi} & \text{inside the slipstream,} \\ 0 & \text{outside the slipstream.} \end{cases} \tag{5}$$

Finally to complete the through-flow differential problem formulation, the conditions at infinity and at the duct boundary [3] have to be associated to equation (5):

$$\frac{1}{\sigma}\frac{\partial\Psi}{\partial\sigma} \to U_\infty, \quad \frac{\partial\Psi}{\partial\zeta} \to 0 \qquad \text{as} \quad \zeta \to -\infty \quad \text{or} \quad \sigma \to \pm\infty, \tag{6a}$$

$$\frac{\partial\Psi}{\partial\zeta} \to 0 \qquad \text{as} \quad \zeta \to +\infty, \tag{6b}$$

$$\Psi = \Psi_0 = const. \qquad \text{on} \quad C, \tag{6c}$$

where C is the duct wall surface.

Summarizing, the solution of the differential through-flow problem is the Stokes stream function induced by an actuator disk with prescribed radial distribution of the load $\mathcal{H}$ and angular velocity Ω that satisfies equation (5). Moreover, the resulting induced axial velocity far away from the slipstream has to approach the free-stream value U_∞ and the radial velocity has to vanish everywhere at infinity (see conditions (6a) and (6b)). Finally, for the ducted configuration, the solution Ψ has to make the duct a stream surface (condition (6c)).

It is noteworthy that the slipstream edge $\sigma_s(\zeta)$, defining the space region outside of which the tangential vorticity vanishes (see equation (4)), is not know in advance and must be computed as a part of the solution of equation (5).

At the end once the through-flow problem has been solved, the tangential velocity induced by the disk can be simply computed through the angular momentum equation

$$\mathcal{H}(\Psi) = H(\Psi) - H_\infty = \Omega\sigma w. \tag{7}$$

With the help of the Hankel transform, it can be shown [39,47] that the stream function of a ring vortex with unit radius r and strength κ is the Green function of the linear elliptic operator on the left-hand side of equation (5). This means that the flow around the ducted actuator disk can be modelled by the superposition of ring vortices [3] each of which induces the following stream function and velocity distributions [48,49]:

$$\frac{\Psi'(\zeta,\sigma)}{\sigma} = \frac{\kappa r}{2}\int_0^\infty \mathrm{e}^{-s|\zeta - z|}\mathrm{J}_1(sr)\mathrm{J}_1(s\sigma)\,\mathrm{d}s, \tag{8}$$

$$u'(\zeta,\sigma) = \frac{\kappa r}{2}\int_0^\infty \mathrm{e}^{-s|\zeta - z|}s\mathrm{J}_1(sr)\mathrm{J}_0(s\sigma)\,\mathrm{d}s, \tag{9}$$

$$v'(\zeta,\sigma) = \pm\frac{\kappa r}{2}\int_0^\infty \mathrm{e}^{-s|\zeta - z|}s\mathrm{J}_1(sr)\mathrm{J}_1(s\sigma)\,\mathrm{d}s. \tag{10}$$

In the above equations, the ring vortex is located at $(\zeta = z, \sigma = 0)$, J is the Bessel function of the first kind and the positive sign is for $\zeta - z \geq 0$ and vice versa.

In more detail, a continuum surface singularity distribution $\gamma_{ad}(\zeta,\sigma)$ can be employed to model the vortical wake region [1], while the flow around the duct can be described through a sheet of ring vortices with density strength $\gamma_d(c)$, where c is the curvilinear abscissa along the duct section profile [2]. Thus, integrating equation (8) over the wake and

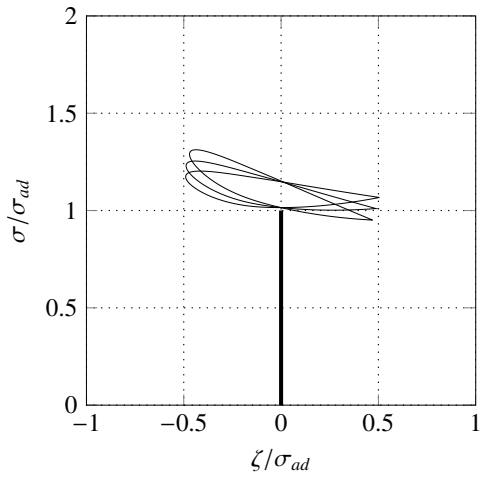

Fig. 1: Propeller ducted with NACA 4415 profiles: duct D1, D2 and D3.

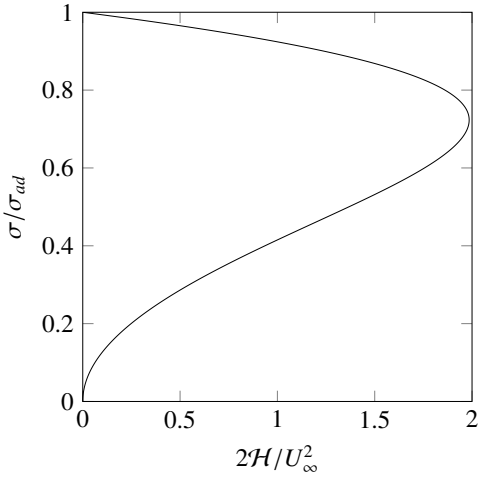

Fig. 2: Propeller ducted with a NACA 4415 profile at $\alpha = 6°$ with $\widehat{b} = 5$ and $J = 0.5$: radial distribution of the load.

the profile leads to the exact solution for the overall flow [3]

$$\frac{\Psi(\zeta,\sigma)}{\sigma} = \underbrace{\frac{1}{2}\int_0^\infty\int_0^{\sigma_s(z)}\int_0^\infty \mathrm{e}^{-s|\zeta-z|}\gamma_{ad}(z,r)r\mathrm{J}_1(sr)\mathrm{J}_1(s\sigma)\,\mathrm{d}s\,\mathrm{d}r\,\mathrm{d}z}_{\frac{\Psi_d(\zeta,\sigma)}{\sigma}} + \frac{1}{2}\oint_C\int_0^\infty \gamma_d(c)r(c)\mathrm{e}^{-s|\zeta-z|}\mathrm{J}_1(sr(c))\mathrm{J}_1(s\sigma)\,\mathrm{d}s\,\mathrm{d}c + \frac{U_\infty\sigma}{2}. \tag{11}$$

The ring vortex strengths γ_{ad} and γ_d have to be such that the resulting overall stream function Ψ satisfies problem (5)-(6). In particular, it can be shown ([3] and reference therein) that $\gamma_{ad}(\zeta,\sigma)$ has to be equal to the θ-component of the vorticity $\omega_\theta(\zeta,\sigma)$ which is related to the radial distribution of the load through equation (4). Moreover, it can be further shown [3] that $\gamma_d(c)$ has to satisfy the following Fredholm integral equation of the second kind:

$$-\frac{1}{2}\gamma_d(c) + \oint_C k(c,\tilde{c})\gamma_d(\tilde{c})\,\mathrm{d}\tilde{c} + (U_\infty + u(c))\cos\beta(c) + v(c)\sin\beta(c) = 0, \tag{12}$$

where $\beta(c)$ is the local profile slope and $k(c,\tilde{c})$ is the velocity parallel to the surface, at c, induced by a ring vortex of unit strength located at $\tilde{c}$. Finally in order to mimic the lifting behaviour of the duct, the $\gamma_d(c)$ distribution has to satisfy the Kutta condition at the trailing edge. Although equation (11) is exact, the Stoke stream function Ψ can not

Table 1: Propeller ducted with a NACA 4415 profile: geometry and operating condition.

chord/σ_{ad}	α			tip gap/σ_{ad}	J
1.0	6.0° duct D1	12.7° duct D2	20.0° duct D3	1.5 %	0.5

be directly evaluated via (11) because of the formulation implicitness.

The iterative and semi-analytical procedure employed to compute the solution Ψ is deeply described in [3] and it is not reported herein for the sake of brevity. The method can handle arbitrary radial distributions of load that can be

Table 2: Propeller ducted with a NACA 4415 profile at $\alpha = 6^\circ$ with $\widehat{b} = 5$ and $J = 0.5$: performance coefficients.

C_T	$C_{T,rot}$	$C_{T,duct}$	C_P	η
1.59	1.26	0.33	2.10	0.76

cast in the following polynomial form:

$$\mathcal{H}(\Psi) = \sum_{m=0}^{M} a_m \left(\frac{\Psi}{\Psi_{\sigma_{ad}}} \right)^m, \tag{13}$$

where $\Psi_{\sigma_{ad}}$ is the stream function at $(\zeta = 0, \sigma = \sigma_{ad})$ and σ_{ad} is the radius of the actuator disk. In the above equation only the quantities a_m constitutes the user defined input parameters to be supplied to the method.

In this paper the following typical definitions are used for the thrust and power coefficients:

$$C_T = \frac{T}{\frac{1}{2}\rho U_\infty^2 \pi \sigma_{ad}^2}, \qquad C_P = \frac{P}{\frac{1}{2}\rho U_\infty^3 \pi \sigma_{ad}^2},$$

where T and P are the magnitude of the thrust and the power experienced by the device. For the ducted propeller the overall thrust can be divided into the duct and the rotor thrust

$$\boldsymbol{T} = \boldsymbol{T}_{rot} + \boldsymbol{T}_{duct},$$

thus obtaining $C_T = C_{T,rot} + C_{T,duct}$. Table 2 lists the performance coefficients for a propeller ducted with a NACA 4415 whose chord makes a $\alpha = 6^\circ$ degree angle with the ζ axis (see Table 1 and Figure 1 for geometrical details). The radial distribution of the load presently adopted is of the following type:

$$\mathcal{H}(\Psi) = a_1 \left[\frac{\Psi}{\Psi_{\sigma_{ad}}} - \left(\frac{\Psi}{\Psi_{\sigma_{ad}}} \right)^2 \right], \tag{14}$$

with the load magnitude parameter $\widehat{b} = \sigma_{ad}^2 a_1 / U_\infty \Psi_{\sigma_{ad}} = 5$. The advance coefficient has been set equal to $J = U_\infty / nD = 0.5$, where n and D are the rotational speed and the propeller diameter, respectively. Despite its simplicity, the radial distribution of the load (Figure 2) obtained with equation (14) has a good physical resemblance with that of a generic propeller.

3. The duct effect: linear and non-linear analysis

As stated in the introduction, ducted propellers are widely diffused devices which are mainly employed to improve the propulsive efficiency of heavily loaded rotors. Significant and meaningful insights into the possibility to obtain an increase of the efficiency can be gained by the one dimensional linearised actuator disk theory with no wake rotation (see for example Von Mises[50], Küchemann and Weber[13] and Oosterveld[10]). With the help of the classical hypothesis of the previously mentioned theory, the magnitude of the work done by the propeller can be expressed as

$$W = \mathcal{H} = \frac{\Delta p_{rot}}{\rho} = \frac{1}{2}(u_e^2 - U_\infty^2). \tag{15}$$

In the above equation, Δp_{rot} is the pressure difference across the rotor and u_e is the wake velocity at infinity downstream. Making use of equation (15), the power absorbed by the propeller reads

$$P = \dot{m} W = \rho u_{rot} A_{rot} \frac{\Delta p_{rot}}{\rho} = u_{rot} T_{rot}, \tag{16}$$

where $A_{rot} = \pi \sigma_{ad}^2$, u_{rot} is the axial velocity at the rotor plane and $T_{rot} = \Delta p_{rot} A_{rot}$ is the magnitude of the rotor thrust. From the axial momentum equation, the expression for the magnitude of the overall thrust can be obtained

$$T = \dot{m}(u_e - U_\infty) = \rho u_{rot} A_{rot} U_\infty (\widehat{u_e} - 1), \tag{17}$$

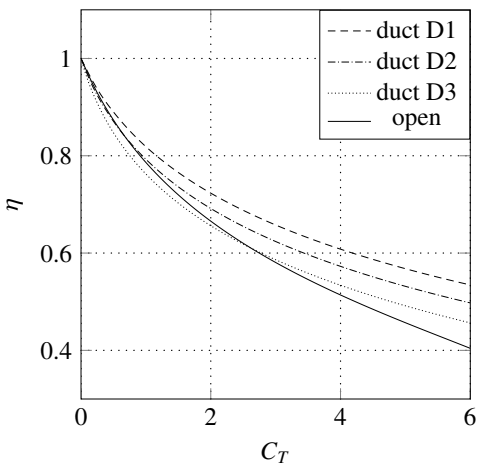

Fig. 3: Efficiency comparison between open and ducted propellers.

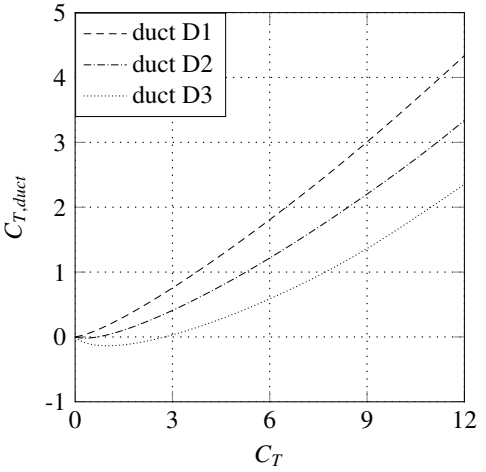

Fig. 4: Duct thrust coefficient for ducted propellers.

where $\widehat{u}_e = u_e/U_\infty$ is the dimensionless wake velocity downstream at infinity. Using equations (15), (16) and (17), the performance coefficients of the device can be cast in the following form:

$$C_{T,rot} = \frac{T_{rot}}{\frac{1}{2}\rho U_\infty^2 A_{rot}} = \frac{2\mathcal{H}}{U_\infty^2} = \widehat{u}_e^2 - 1, \tag{18}$$

$$C_T = \frac{T}{\frac{1}{2}\rho U_\infty^2 A_{rot}} = 2\widehat{u}_{rot}(\widehat{u}_e - 1), \tag{19}$$

$$C_P = \frac{P}{\frac{1}{2}\rho U_\infty^3 A_{rot}} = \widehat{u}_{rot} C_{T,rot} = \frac{C_T}{2}(\widehat{u}_e + 1). \tag{20}$$

Finally, the propulsive efficiency is

$$\eta = \frac{C_T}{C_P} = \frac{2}{\widehat{u}_e + 1} = \frac{2}{1 + \sqrt{1 + C_{T,rot}}}. \tag{21}$$

The aim of the duct is to increase the efficiency for a prescribed propulsive thrust required by the carrier. Therefore, from equation (21), it is clear that this result is achieved decreasing the rotor thrust, while the missing axial force must be delivered by the duct. In fact, in order to keep constant the overall propulsive thrust of the device (given by $\boldsymbol{T} = \boldsymbol{T}_{rot} + \boldsymbol{T}_{duct}$), the duct must be designed in such a way that $\boldsymbol{T}_{duct}$ and $\boldsymbol{T}_{rot}$ have the same direction. Conversely, if the direction of $\boldsymbol{T}_{duct}$ is opposite to that of the $\boldsymbol{T}_{rot}$, then the latter has to be increased with a consequent drop in the efficiency. At the end, it is noteworthy that the duct improves the efficiency by reducing the rotor load, but increasing the mass flow rate swallowed by the propeller. In fact from equation (18) a decrease in the rotor thrust implies a decrease in the wake velocity downstream at infinity which, the total thrust in equation (17) being constant, leads to an increase in the mass flow rate.

Turning now to the more accurate and realistic non-linear actuator disk theory described in §2, Figure 3 shows the comparison between the propulsive efficiency of the ducted propellers described in Table 1 and the open propeller at different values of C_T. In particular, the open propeller results are obtained with the same load radial distribution type (equation (14)) and advance coefficient of the ducted propellers. Figure 4 presents the thrust coefficient of the ducts of Table 1 at different values of C_T; as customary the $C_{T,duct}$ coefficient is considered positive (negative) if $\boldsymbol{T}_{duct}$ and $\boldsymbol{T}_{rot}$ have the same (opposite) direction. As showed in Figure 3, the propellers equipped with the duct D1 is characterised by an higher efficiency, regardless of the C_T value. This is due to the positiveness of $C_{T,duct}$ for all C_T (see Figure 4). Otherwise ducts D2 and D3, for small C_T values, exert an axial force with opposite direction in comparison to the

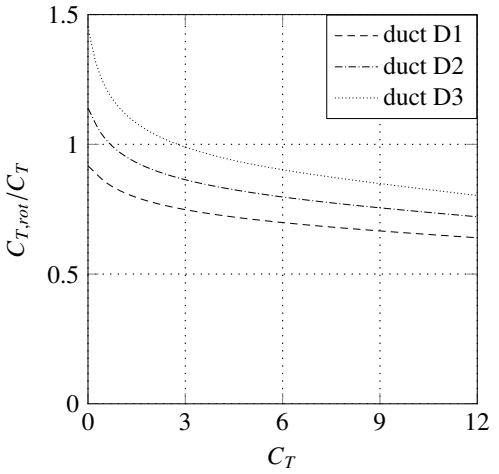

Fig. 5: Rotor thrust contribution to the overall propulsive thrust for ducted propellers.

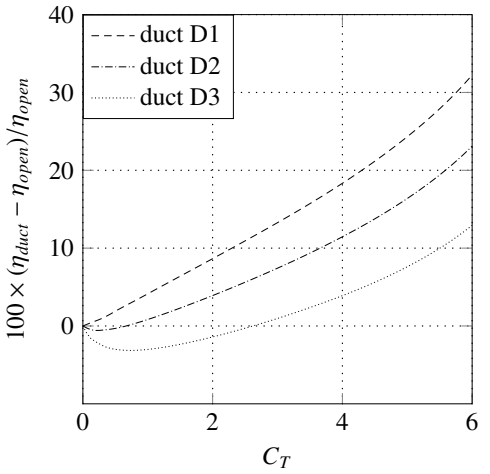

Fig. 6: Percentage variation in efficiency for ducted and open propellers.

rotor thrust thus obtaining, in accordance with the linearised theory, a lower efficiency compared with that of the open propeller. Furthermore, the relative contribution of the duct to the propulsive thrust becomes larger and larger as the overall thrust increases (see Figure 5). Consequently, compared with the open propeller, the efficiency increases as well (see Figure 6).

Another very important aspect that deserves to be investigated is the appropriate matching between the rotor and the duct at different operating conditions. In particular, as already stated, the duct shape and its arrangement have to be devised as to increase the efficiency. From this point of view, it is essential to avoid flow separation on both sides (inner and outer) of the duct which is likely to occur for heavily loaded nozzles at off-design conditions. In more detail, if the rotor load and consequently the mass flow swallowed by the propeller are much lower (larger) than the design one, then the front stagnation point is located on the internal (external) surface of the duct thus promoting flow separation on the external (internal) surface. The displacement of the stagnation point in the leading edge region as the load is changed is clearly visible in Figure 7 reporting the stagnation streamlines for duct D2 at different C_T values. Figure 8 shows instead the wall pressure coefficient $C_{p,w} = (p - p_\infty)/\frac{1}{2}\rho U_\infty^2$ distribution for duct D2 at different values of C_T. As anticipated, for high and low values of the rotor load the $C_{p,w}$ profiles point out the presence of undesired velocity peaks that could lead to flow separation. Always with reference to duct D2, the value of C_T for which the leading edge is unloaded (optimum incidence) is $C_T \approx 5.59$.

On the other side, from a design point of view, if the target C_T value is significantly higher or lower than $C_T = 5.59$, then the geometry of the duct should be changed in order to prevent flow separation. One way to overcome this problem is to modify the angle α between the profile chord and the ζ axis for a prescribed shape of the profile itself (see Table 1 and Figure 1). For $C_T < 5.59$ a duct with a lower value of the α angle should be employed and vice versa. In fact, for ducts D1 and D3 the optimum incidences are those associated to the following C_T values: $C_T \approx 1.59 < 5.59$ and $C_T \approx 8.71 > 5.59$.

4. Conclusions

A generalised semi-analytical actuator disk model, which strongly couples the actuator disk theory of Conway[1] and the the vortex element method of Martensen[2], has been employed to analyse the flow around open and ducted propellers. In particular, the method has been shown capable to deal with ducts of general shape, and rotors with variable distribution of the load and wake rotation. The analysis of the results about ducted propellers with different values of the rotor load have shown that, in order to increase the device efficiency for prescribed propulsive thrust, the duct must be properly designed. In more detail, according to the linearised theory, the coupling between the duct

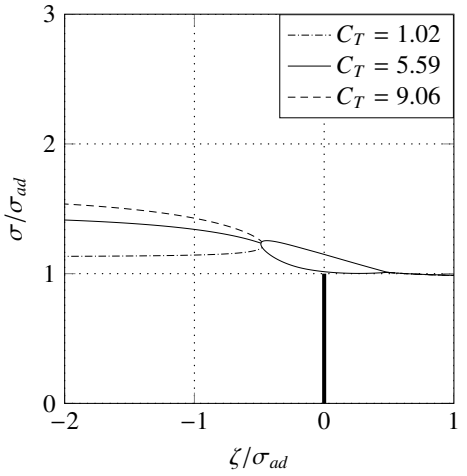

Fig. 7: Streamlines for duct D2 at different values of the thrust coefficient C_T.

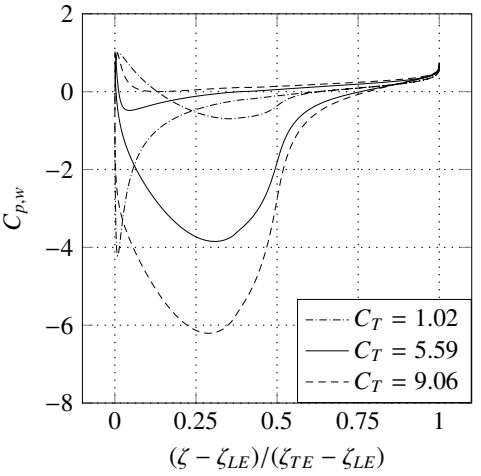

Fig. 8: Wall pressure coefficient for duct D2 at different values of the thrust coefficient C_T.

and the rotor has to return a lower rotor load, i.e. $\boldsymbol{T}_{duct}$ and $\boldsymbol{T}_{rot}$ need to have the same direction. Furthermore, the beneficial effect of the duct is shown to be particularly significant for heavily loaded propellers. Finally, the method has been successfully employed to properly match the duct and the rotor, the optimal matching being based on the analysis of the local flow characteristics occurring in the duct leading edge region.

The computer code is freely available on contacting the authors.

Acknowledgements

The authors would like to thank Professor S. Miranda for his helpful suggestions.

References

[1] Conway, J.T.. Exact actuator disk solutions for non-uniform heavy loading and slipstream contraction. J Fluid Mech 1998;365:235–267.
[2] Martensen, E.. Berechnung der druckverteilung an gitterprofilen in ebener potentialstromung mit einer fredholmschen integralgleichung. Arch Rat Mech 1959;3:235 – 270.
[3] Bontempo, R., Manna, M.. Solution of the flow over a non-uniform heavily loaded ducted actuator disk. Journal of Fluid Mechanics 2013;728:163–195. URL: http://journals.cambridge.org/article_S0022112013002577. doi:10.1017/jfm.2013.257.
[4] Stipa, L.. Ala a turbina. L'Aerotecnica 1931;:923–953.
[5] Kort, L.. Der neue düsenschrauben-antrieb. Werft, Reederei und Hafen 1934;15.
[6] Van Manen, J.D.. Recent research on propellers in nozzles. International Shipbuilding Progress 1957;4(36).
[7] Van Manen, J.D., Superina, A.. The design of screw propellers in nozzles. International Shipbuilding Progress 1959;6(55):95–113.
[8] Van Manen, J.D.. Effect of radial load distribution on the performance of shrouded propellers. Transaction RINA 1962;.
[9] Van Manen, J.D., Oosterveld, M.W.C.. Analysis of ducted propeller design. Transaction SNAME 1966;74:522–561.
[10] Oosterveld, M.W.C.. Wake adapted ducted propellers. Tech. Rep. 345; Netherlands Ship Model Basin; 1970.
[11] Horn, F.. Beitrag zur theorie ummantelter schiffsschrauben. Jahrbuch der schiffbautechnischen Gesellschaft 1940;:106–187.
[12] Horn, F., Amtsberg, H.. Entwurf von schiffsdüsen systemen (kortdüsen). Jahrbuch der schiffbautechnischen Gesellschaft 1950;44:141–206.
[13] Küchemann, D., Weber, J.. Aerodynamics of propulsion. McGraw-Hill; 1953.
[14] Tachmindji, A.J.. The potential problem of the optimum propeller with finite number of blades operating in a cylindrical duct. Journal of Ship Research 1958;2(3):23–32.
[15] Ordway, D.E., Sluyter, M.M., Sonnerup, B.O.U.. Three-dimensional theory of ducted propellers. 1960.
[16] Morgan, W.B.. A theory of the ducted propeller with a finite number of blades. Tech. Rep.; University of California, Berkeley, Institute of engineering research; 1961.
[17] Morgan, W.B.. Theory of the annular airfoil and ducted propeller. In: Proceedings of the Fourth Symposium on Naval Hydrodynamics. 1962, p. 151–197.

[18] Dyne, G.. A method for the design of ducted propellers in a uniform flow. Tech. Rep. 62; SSPA; 1967.
[19] Ryan, P.G., Glover, E.J.. A ducted propeller design method: a new approach using surface vorticity distribution techniques and lifting line theory. Trans RINA 1972;114:545 – 563.
[20] Morgan, W.B., Caster, E.B.. Comparison of theory and experiment on ducted propellers. In: Cooper, R.D., Doroff, S.W., editors. Proceedings of the 7th Symposium on Naval Hydrodynamics. 1968, p. 1311–1349.
[21] Caracostas, N.. Off design performance analysis of ducted propellers. In: Proceedings Propellers/Shafting '78 Symposium, SNAME. 1978, p. 3.1–3.8.
[22] Tsakonas, S., Jacobs, W.R., Ali, M.R.. Propeller-duct interaction due to loading and thickness effects. In: Proceedings of the Propellers/Shafting '78 Symposium, SNAME. 1978,.
[23] Van Houten, R.. Analysis of ducted propellers in steady flow. Tech. Rep.; Airflow Research and Manufacturing Corp.; 1986.
[24] Kerwin, J.E., Kinnas, S.A., Lee, J.T., Shih, W.. A surface panel method for the hydrodynamic analysis of ducted propellers. Trans SNAME 1987;95.
[25] Kinnas, S.A., Coney, W.B.. On the optimum ducted propeller loading. In: Proceedings Propellers '88 Symposium. 1988, p. 1.1–1.13.
[26] Coney, W.B.. A method for the design of a class of optimum marine propulsors. Ph.D. thesis; Massachusetts Institute of Technology; 1989.
[27] Kinnas, S.A., Coney, W.B.. The generalised image model - an application to the design of ducted propellers. Journal of Ship Research 1992;36:197–209.
[28] Baltazar, J., Falcão de Campos, J.A.C.. On the modelling of the flow in ducted propellers with a panel method. In: Proceedings of the 1st International Symposium on Marine Propulsors; vol. 9. 2009,.
[29] Çelik, F., Güner, M., Ekinci, S.. An approach to the design of ducted propeller. Transaction B: Mechanical Engineering, Scientia Iranica 2010;17(5):406–417.
[30] Abdel-Maksoud, M., Heinke, H.J.. Scale effects on ducted propellers. In: Proceedings of the 24th Symposium on Naval Hydrodynamics. 2002,.
[31] Kim, J., Paterson, E., Stern, F.. Sub-visual and acoustic modeling for ducted marine propulsor. In: Proceedings of the 8th International Conference on Numerical Ship Hydrodynamics. 2003, p. 22–25.
[32] Wang, T., Zhou, L.D., Zhang, X.. Numerical simulation of 3-d integrative viscous complicated flow field around axisymmetric body with ducted propulsion. Journal of Ship Mechanics 2003;7(2):21–32.
[33] Hoekstra, M.. A rans-based analysis tool for ducted propeller systems in open water condition. International shipbuilding progress 2006;53(3):205–227.
[34] Sánchez-Caja, A., Pylkkänen, J.V., Sipilä, T.P.. Simulation of the incompressible viscous flow around ducted propellers with rudders using a ranse solver. In: Proceeding of the 27th Symposium on Naval Hydrodynamics. 2008,.
[35] Haimov, H., Vicario, J., Del Corral, J.. Ranse code application for ducted and endplate propellers in open water. In: Proceedings of the Second International Symposium on Marine Propulsors. 2011,.
[36] Rankine, W.J.M.. On the mechanical principles of the action of propellers. Trans Inst Nav Arch 1865;6.
[37] Froude, R.E.. On the part played in propulsion by differences of fluid pressure. Transactions of the Institute of Naval Architects 1889;30:390–405.
[38] Conway, J.T.. Analytical solutions for the actuator disk with variable radial distribution of load. J Fluid Mech 1995;297:327–355.
[39] Wu, T.Y.. Flow through a heavily loaded actuator disc. Schiffstechnik 1962;9:134 – 138.
[40] Greenberg, M.D., Powers, S.R.. Nonlinear actuator disk theory and flow field calculations, including nonuniform loading. Tech. Rep. CR-1672; NASA; 1970.
[41] Dickmann, H.E., Weissinger, J.. Beitrag zur theorie optimaler dusenchrauben (kortdusen). Schiffbautrchn 1955;49:452–486.
[42] Chaplin, H.. A method for numerical calculation of slipstream contraction of a shrouded impulse disk in the static case with application to other axisymmetric potential flow problems. Tech. Rep. 1857; David Taylor Model Basin; 1964.
[43] Van Gunsteren, L.A.. A contribution to the solution of some specific ship propulsion problems. Ph.D. thesis; Delft University of Technology; 1973.
[44] Gibson, I.S., Lewis, R.I.. Ducted propeller analysis by surface vorticity and actuator disk theory. In: Proceedings of the Symposium on Ducted Propeller. Royal Institute of Naval Architects; 1973,.
[45] Falcão de Campos, J.A.C.. On the calculation of ducted propeller performance in axisymmetric flows. Ph.D. thesis; Delft University of Technology; 1983.
[46] Batchelor, G.K.. An intoduction to fluid dynamics. Cambridge University Press; 1967.
[47] Breslin, J.P., Andersen, P.. Hydrodynamics of ship propellers. Cambridge University Press; 1994.
[48] Basset, A.B.. A treatise on hydrodynamics. vol. II. Deighton Bell; 1888.
[49] Lamb, H.. Hydrodynamics. Cambridge University Press; 1932.
[50] Von Mises, R.. Theory of flight. McGraw-Hill; 1945.